Unified one-dimensional model of bounded plasma with nonzero ion temperature in a broad pressure range

J. H. Palacio Mizrahi, V. Tz. Gurovich, and Ya. E. Krasik
Physics Department, Technion, Haifa 32000, Israel

(Received 14 November 2012; accepted 7 March 2013; published online 29 March 2013)

A one-dimensional model for steady state plasmas bounded either between large parallel walls, or by a cylinder or a sphere, valid in a wide range of gas pressures, is considered. The model includes nonzero ion temperature, inertial terms in the ion momentum equations, and allows one to calculate the plasma electron temperature and ion current density reaching the wall, as well as the spatial distributions of the ion fluid velocity, plasma density, and plasma potential in the plasma bulk. In addition, the effect of electron inertia is analyzed. The model includes as particular cases several earlier models that were based on a similar set of differential equations, but that are restricted to a specific pressure regime (low, intermediate, or high). Analytical solution is found in planar geometry, and numerical solution is given in cylindrical and spherical geometry. The results obtained are compared with those of earlier models and the differences are analyzed. © *2013 American Institute of Physics*. [http://dx.doi.org/10.1063/1.4798401]

I. INTRODUCTION

Non magnetized low-ionized plasma, bounded either between parallel walls with sides larger than the distance between them, or inside a cylinder whose length is much larger than its radius, or inside a sphere, can be described in the fluid approximation by the self-consistent solution with appropriate boundary conditions of the steady state 1D-continuity and momentum equations for plasma ions and electrons along with the Poisson equation. If only the plasma bulk is to be considered, then quasi-neutrality can be assumed and the Poisson equation can be omitted.[1] If inertial terms are not neglected in the ion momentum equation, then a plasma-sheath boundary can be defined.[2,3]

Several solutions, both analytical and numerical, of the 1D-fluid equations describing bounded plasmas have been obtained, assuming either zero ion temperature (cold ions approximation)[4,5] or constant nonzero ion temperature.[3,6] The solutions for the distribution of the plasma parameters have been found separately in the low, intermediate, and large pressure regimes,[3,5,7] and heuristic arguments,[5,8–10] or combined models of ion neutral collision frequency[6,8,9,11] have been used to join these solutions. Models that analyze the depletion of neutral atoms[2,12,13] have also been developed based on the same fluid equations. The plasma electron temperature is commonly determined from an eigenvalue equation obtained from the balance between ion generation and ion losses but usually neglecting the ion inertia.

In the present paper, the problem of bounded plasmas is solved for planar, cylindrical, and spherical geometries assuming plasma quasi-neutrality. The effect of constant nonzero ion temperature on the plasma parameters is analyzed, and the electron temperature T_e is determined taking into account the ion inertia. The obtained solution is valid in a broad range of the pressures commonly used in gas discharges. Additionally, an approximated analytical solution is found in the case of planar geometry. It is shown that the plasma density at the plasma-sheath boundary is lower than that predicted by the variable mobility model[5] in which the ion inertia is neglected. Comparison with the most updated model by Curreli and Chen[2] is made, and it is shown that a nonzero ion temperature can change considerably the plasma density and potential distributions while retaining the same form of these distributions. The influence of the electron inertia and electron-neutral collisions on the plasma parameters behavior is also analyzed.

II. OVERVIEW OF EARLIER 1D-PLASMA MODELS

In 1928, Tonks and Langmuir[4] presented a one-dimensional (1D) model for the potential and density distributions of steady state plasmas in contact with an absorbing wall. In this model, a so-called complete plasma-sheath equation was derived and solved numerically for planar, cylindrical, and spherical geometries. The ion generation rate $\dot{n}$ was considered either proportional to the plasma electron density or uniform throughout the plasma.[4,14] The model was solved in the low (free fall theory), intermediate, and large gas pressures regimes, and quasi-neutrality was not assumed. The pressure regime is determined by the ratio L/λ_i, where L is the characteristic plasma size and λ_i is the ion mean free path for collision with neutrals. The intermediate pressure regime corresponds to $L/\lambda_i \sim 1$, while the low and high pressure regimes correspond to $L/\lambda_i \ll 1$ and $L/\lambda_i \gg 1$, respectively. In the high pressure regime, it was shown that the solution of the model coincides with the solution of the Schottky ambipolar diffusion model.[7] The Tonks-Langmuir model allows one to distinguish between two different regions, namely, a quasi-neutral region, which is called the plasma bulk, and the sheath region which is positively charged. The boundary between these regions was defined as the location at which the plasma potential and density, while remaining finite, have infinite gradients. The solutions were found using the Poisson and momentum equations and assuming cold ions ($T_i = 0$). The plasma electrons were supposed to have a Boltzmann distribution in space,

which is equivalent to neglect inertial and collision terms in the electron momentum equation. In the low pressure regime, the collision term $Mn_i\nu_{in}u_i$ and the linear inertial term $M\dot{n}u_i$ in the ion momentum equation (see Eq. (2) in Sec. III) were neglected, while the nonlinear inertial term $Mn_iu_idu_i/dx$ was retained. Here M, n_i, u_i, and ν_{in} are the ion mass, ion density, ion fluid velocity, and ion-neutral collision frequency, respectively. In the high pressure regime, both inertial terms were neglected and the collision terms were retained in the ion momentum equation. Thus, this model does not allow one to obtain a general solution that can be applied in both pressure regimes.

In 1966, Self and Ewald[3] presented a model to describe the plasma density and potential distributions in the entire range of pressures. Also this model is based on solutions of the momentum and continuity equations for electrons and ions, and quasi-neutrality is assumed. In the electron momentum equation, the nonlinear inertial term $m_en_eu_edu_e/dx$ was neglected, but the total momentum equation for ions was considered (viscous effects were also neglected, as was in the Tonks-Langmuir model). Here, m_e, n_e, and u_e are the electron mass, density, and fluid velocity, respectively. The model has an analytical solution in the case of planar geometry. In the high pressure regime, the results of this model are similar to those predicted by the Schottky model,[7] and at low pressure, they differ only slightly from those of the free fall model of Tonks and Langmuir.[4] It should be noted that this model considers a constant ion-neutral collision frequency at all pressures, which in fact cannot be a correct assumption.[3,5,9]

In 1986, Godyak reported in Ref. 5 a plasma model that considers the ion-neutral collision frequency to be proportional to the ion fluid velocity (variable mobility model) instead of to the ion thermal velocity. In this model, the plasma electrons are assumed to have a Boltzmann distribution, the ions are assumed to be cold, and both inertial terms are neglected in the plasma ion momentum equation. In the case of planar geometry, this model has an analytical solution that is valid at intermediate pressures. By using heuristic arguments, solutions for the plasma density distribution were obtained separately for the cases of low and high pressure regimes. In 1995, Lee and Lieberman[9,10] found an expression for the plasma density distribution in their research of high-density plasma discharges that is similar to that found by Godyak.[5]

In 1953, Wannier[15] introduced a model for the ion-neutral collision frequency, which he proposed as appropriate to describe the ion-neutral interaction at intermediate pressures. This model was used by Sternovsky and Robertson in Ref. 6 to describe the decrease in ion current density toward the wall caused by the plasma collisionality. In Ref. 6, the change in the ion-neutral collisionality experienced by the plasma ions propagating through the plasma toward the wall was taken into account. This model considered a finite temperature for the plasma ions, but with the restriction $T_i/T_e \equiv \tau \leq 0.1$ because the ion pressure gradient term in the ion momentum equation was neglected.

In 2007, Chabert *et al.*,[11] in a study on expanding electronegative plasma, introduced a model for the ion-neutral collision frequency at intermediate pressures, which is essentially the same as that proposed by Wannier. The specific form of the expression for the ion-neutral collision frequency used by Sternovksky and Robertson[6] differs from that used by Chabert *et al.*[11] by a factor of $\sqrt{2}$ in the ion thermal velocity.

In 2011, Curreli and Chen have developed a model[2] for a plasma discharge with cylindrical symmetry, which accounts for ion inertia, neutral depletion, and local power deposition. In Ref. 2, the model is solved first by considering radially constant neutral density and electron temperature (neglecting the diffusive term $k_BT_i\nabla n$ in the ion momentum equation), which leads to a "universal" profile of ion velocity, plasma density, and plasma potential in the sense that distributions of the plasma parameters do not depend neither on the cylinder radius nor on the neutral density nor on the ionization degree at the cylinder axis.

III. DESCRIPTION OF THE MODEL

The present model considers 1D steady state plasmas bounded by either parallel plates whose sides are larger than the distance between them, or a cylinder with a length much larger than the radius, or a sphere, in such a way that the only relevant dynamic of the plasma particles is in the direction perpendicular to the walls. The distance between the plates or the diameter of the cylinder and the sphere is $2L$, and the origin of the system of coordinates is at the middle distance between the plates, at the cylinder axis, or at the sphere center, respectively.

It will be supposed that the neutral atoms are ionized in a single event by electron impact, and that the ion generation rate is given by $\dot{n} = \nu_{iz}n_e$, where $\nu_{iz} = n_0\langle\sigma_{iz}u_{e,th}\rangle$ is the ionization frequency. Here, n_0 is the neutral density, $\sigma_{iz}(u^2_{e,th})$ is the ionization cross section of neutrals by electron impact which depends on the kinetic energy of the electron, $u_{e,th}$ is the thermal velocity of the plasma electrons, which are supposed to have a distribution function $g_{T_e}(u^2_{e,th})$ at electron temperature T_e, and the brackets signify averaging over the distribution: $\langle\sigma_{iz}u_{e,th}\rangle = \int_0^\infty \sigma_{iz}(u^2)ug_{T_e}(u^2)du$. It is also supposed that the plasma ions are at the same temperature, $T_i = T_0 = \text{const}$, as the neutral gas background.

The equations are solved for the plasma bulk where the condition of quasi-neutrality $n_e = n_i \equiv n$ can be assumed. The momentum and continuity equations for the plasma electrons and ions are

$$m_e\left[n\nu_{iz}u_e + nu_e\frac{du_e}{dx}\right] = -enE - k_BT_e\frac{dn}{dx} - m_en[\nu_{ei}(u_e - u_i) + \nu_{en}(u_e - u_n)], \quad (1)$$

$$M\left[n\nu_{iz}u_i + nu_i\frac{du_i}{dx}\right] = enE - k_BT_i\frac{dn}{dx} - Mn\nu_{in}(u_i - u_n), \quad (2)$$

$$\frac{1}{x^\beta}\frac{d(x^\beta nu_e)}{dx} = \frac{1}{x^\beta}\frac{d(x^\beta nu_i)}{dx} = n\nu_{iz}. \quad (3)$$

Here, u_n is the neutral fluid velocity; $E = -d\varphi/dx$ is the electric field, and φ is the plasma potential; e and k_B are the

electron charge and Boltzmann constant respectively; ν_{en}, ν_{ei}, and ν_{in} are the elastic collision frequencies for electron-neutral, electron-ion, and ion-neutral momentum transfer, respectively; and $\beta = 0, 1, 2$ is the coefficient for planar, cylindrical, and spherical geometry, respectively. The fluid velocity of neutrals is assumed to be negligible, $u_n \approx 0$, which is a reasonable assumption for low-ionized plasmas. In addition, one can show that Eq. (3) implies $u_e = u_i$, and therefore elastic electron-ion collisions ν_{ei} do not affect the ion drift. The ion-neutral collision frequency to be considered is given by[6]

$$\nu_{in} = \frac{1}{\lambda_i}\sqrt{2\bar{u}_{i,th}^2 + (\pi^2/4)u_i^2}. \tag{4}$$

Here, $\bar{u}_{i,th} \equiv \langle u_{i,th}\rangle = \sqrt{8k_BT_i/(\pi M)}$ is the average ion thermal velocity, and $\lambda_i \approx (n_0\sigma_{in})^{-1}$ is the ion mean free path, where σ_{in} is the cross section for ion-neutral interaction. At low ion energies, the cross section for ion-neutral charge exchange (cex) σ_{cex} is approximately constant and larger than that for ion-neutral momentum transfer, and therefore one can use in that case $\sigma_{in} \approx \sigma_{\mathrm{cex}}$. The expression given in Eq. (4) for ν_{in} was suggested in Ref. 15 to describe appropriately the ion-neutral collisionality in the regime of intermediate pressure; it reduces to the correct limits in the low and large pressure regimes. In the low pressure regime, the appropriate limit is given by the so-called variable mobility model[5] in which $T_i = 0$ is supposed, and the ion-neutral collision frequency $\nu_{in} = \pi u_i/(2\lambda_i)$ is proportional to the ion fluid velocity. In the high pressure regime, the appropriate limit is given by the diffusion model,[7] which considers $T_i = T_0$, i.e., the plasma ions are in thermal equilibrium with the neutral gas background, and $u_i \ll \bar{u}_{i,th}$; in that case, the ion-neutral collision frequency[6] $\nu_{in} = \sqrt{2}\bar{u}_{i,th}/\lambda_i$ is proportional to the relative velocity between ions and neutral atoms.

Using the Bohm velocity $u_B = \sqrt{k_B(T_e + T_i)/M}$, the normalized ion fluid velocity $u = u_i/u_B$, and the ratios $\tau \equiv T_i/T_e$, $\theta \equiv (64/\pi^3)\tau/(1+\tau) \cong 2\tau/(1+\tau)$, one can rewrite Eq. (4) as

$$\nu_{in} = \frac{\pi u_B}{2\lambda_i}\sqrt{\theta + u^2}. \tag{5}$$

Because $\nu_{iz} \ll \nu_{en}$, the linear inertial term $m_e n\nu_{iz}u_e$ in Eq. (1) is negligible when compared with the collision term $m_e n\nu_{en}u_e$, and this, along with the relations $m_e \ll M$ and $\nu_{en} \ll \nu_{in}$, allows one to write Eqs. (1)–(3) in the form

$$\frac{du}{ds} = \frac{1 + u^2 + cu^2\sqrt{\theta + u^2} - \beta u/s}{1 - u^2}, \tag{6}$$

$$\frac{1}{h}\frac{dh}{ds} = -\frac{2u + cu\sqrt{\theta + u^2} - \beta u^2/s}{1 - u^2}, \tag{7}$$

$$\frac{d\chi}{ds} = \frac{1}{h}\frac{dh}{ds} + \delta(1+\tau)u + \frac{m_e}{M}(1+\tau)u\frac{du}{ds}. \tag{8}$$

Here, the coordinate $s = \nu_{iz}x/u_B$, the parameters $\delta = (m_e/M)(\nu_{en}/\nu_{iz})$, and $c = \pi u_B/(2\lambda_i\nu_{iz})$, and the normalized plasma density $h(s) = n(s)/n(0)$ and plasma potential $\chi = e\varphi/(kT_e)$ have been introduced. Here, $n(0)$ is the plasma density at the origin of coordinates. The third term in the right hand side of Eq. (8) corresponds to the nonlinear inertial term $m_e n u_e du_e/dx$ in the electron momentum equation and does not contribute appreciably to the solution of the equation for the plasma potential, and can be neglected (see Sec. VI). The second term in the right hand side of Eq. (8) will be analyzed later. The parameter δ is proportional to the elastic electron-neutral collision frequency and appears only in Eq. (8); therefore elastic electron-neutral collisions affect only the plasma potential.

The parameters c and δ depend on the type of gas and on the electron temperature, which in turn is related to the gas pressure p and the geometry of the problem under consideration. By defining $\langle\tilde{\sigma}\rangle \equiv \langle\sigma u_{th}\rangle/\bar{u}_{th}$, one can see that $c \propto \sqrt{m_e/M}(\sigma_{in}/\langle\tilde{\sigma}_{iz}\rangle) \approx \sqrt{m_e/M}(\sigma_{\mathrm{cex}}/\langle\tilde{\sigma}_{iz}\rangle)$ and $\delta = (m_e/M)\langle\tilde{\sigma}_{en}\rangle/\langle\tilde{\sigma}_{iz}\rangle$. The cross section for ionization of neutral atoms $\langle\tilde{\sigma}_{iz}\rangle$ decreases steeply with decreasing electron temperature; therefore, the parameters c and δ tend to be very large at low electron temperature, or equivalently at high pressures (because the value of T_e decreases with increasing pressure). Additionally, one can see that $\delta/c \sim \sqrt{m_e/M}\langle\tilde{\sigma}_{en}\rangle/\sigma_{\mathrm{cex}}$, implying $\delta/c \ll 1$. In the high pressure regime, $\delta \ll c$ because ion-neutral charge exchange collisions are more frequent than elastic electron-neutral collisions. In the low pressure regime, $\delta \ll c$ because the electron temperature is high and this reduces the electron-neutral cross section.

One can see that Eq. (6) is a differential equation for the ion fluid velocity decoupled from any other variable plasma parameter. Analysis of Eq. (6) shows that when $u \to 1$, i.e., when the ion fluid velocity approaches the Bohm velocity, the derivative du/ds diverges to infinite, which is not a physical result. It defines the plasma boundary, i.e., as the plasma boundary is approached, the assumption of the model regarding plasma quasi-neutrality is not fulfilled.[3]

IV. DETERMINATION OF PLASMA PARAMETERS

The plasma boundary is located at $x_b < L$. Assuming the plasma sheath is thin, one can use the approximation $x_b \approx L$ to estimate $s_b \approx L\nu_{iz}/u_B$ and $L/\lambda_i \approx 2cs_b/\pi$. The value of s_b is obtained by solving Eq. (6) for $0 \le u \le 1$. This allows one to find the dependence of c on L/λ_i. In Fig. 1, this dependence is shown for the case of parallel plates ($\beta = 0$). Qualitatively similar behavior is found in the case of cylindrical ($\beta = 1$) and spherical ($\beta = 2$) configurations.

The dependence shown in Fig. 1 for the planar case, and the similar ones for the cylindrical and spherical cases, allow a given value of the parameter c to be identified with a pressure regime. The plasma parameters are determined for known values of $\tau = T_i/T_e$, plasma size L, and neutral pressure p_0, as follows. The relation $s_b \approx L\nu_{iz}/u_B$ can be rewritten in the form

$$s_b \approx Lp_0\langle\sigma_{iz}u_{e,th}\rangle\sqrt{M}/\left((k_BT_e)^{3/2}\tau\sqrt{1+\tau}\right). \tag{9}$$

The electron temperature is estimated by using Eqs. (6) and (9) along with $c = \pi\sigma_{in}\sqrt{k_BT_e(1+\tau)/M}/(2\langle\sigma_{iz}u_{e,th}\rangle)$. Then, it is possible to calculate the parameters $T_i = \tau T_e$, and

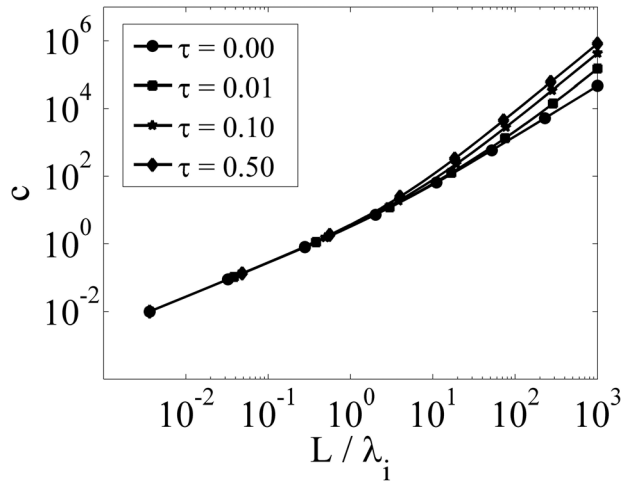

FIG. 1. Dependence of the parameter c on L/λ_i for different values of $\tau \equiv T_i/T_e$ (planar case).

$n_0 = p_0/(k_B T_i)$. The distribution of normalized fluid velocity u, plasma density h, and plasma potential χ is obtained by solving Eqs. (6)–(8) and is shown in Fig. 2 for the planar case.

In Fig. 2, one can see that in the high pressure regime ($L/\lambda_i \gg 1$), the ion fluid velocity increases slowly from the center of the plasma, and the ion fluid experiences strong acceleration only very near to the sheath boundary in order to reach the Bohm velocity. The slow increase in the ion fluid velocity in the plasma bulk occurs due to the large ion-neutral collision frequency and low potential drop. Close to the sheath boundary, the potential falls more steeply, causing ion acceleration, which in turns leads to a decrease in the plasma density. In the low pressure regime ($L/\lambda_i \ll 1$), the ion-neutral collision frequency is low. Thus, a smaller potential difference is required in order to accelerate the ions to the Bohm velocity at the sheath boundary.

The influence of the non-zero ion temperature on the plasma parameters is shown in Fig. 3. One can see that the ion fluid velocity distribution remains almost unchanged for $0 \le \tau \le 0.5$, while the distributions of the plasma potential and density change significantly, namely, these distributions change more steeply with the increase in τ. One can explain this result as the necessity of a stronger electric field at $T_i > 0$ in order to give to the ions a directed fluid velocity toward the wall.

In the cases of cylindrical and spherical geometry, the behavior of the normalized ion fluid velocity, plasma density, and plasma potential is qualitatively similar to that exhibited in the planar case shown in Figs. 2 and 3.

V. PLASMA PARAMETERS AT THE PLASMA-SHEATH BOUNDARY

The ion fluid velocity at the plasma-sheath boundary is the Bohm velocity $u_i = u_B$, which is equivalent to the normalized ion fluid velocity $u_b = 1$ at the plasma sheath boundary. The location of the (normalized) plasma-sheath boundary s_b and the boundary values of the plasma density h_b and potential χ_b depend on the pressure regime and on the geometry as is shown in Fig. 4.

In Fig. 4(c), the value of the parameter $\delta = (m_e/M)(\nu_{en}/\nu_{iz})$ was taken to be zero. The behavior of χ_b for $\delta \neq 0$ will be analyzed later. Let us recall here that the parameter δ affects only the plasma potential distribution (see Eqs. (6)–(8)). The ion current density at the sheath boundary is determined as $J_{i,b} = en_b u_B = en(0)u_B h_b$, which is equivalent to $h_b = J_{i,b}/(en(0)u_B)$. Therefore, Fig. 4(b) represents the normalized ion current density entering the sheath region. This current density is strongly reduced at high pressures ($L/\lambda_i \gg 1$) due to the increase in plasma collisionality. A similar result was obtained by Sternovsky and Robertson (see Ref. 6 Fig. 1) for the case of homogeneous ($\dot{n} = \text{Const}$) ionization in the plasma bulk.

The effect of a finite ion temperature on the plasma parameters at the plasma-sheath boundary is shown in Fig. 5. One can see that at a fixed ion mean free path ($L/\lambda_i = \text{const}$), the plasma density h_b decreases and the absolute value of the plasma potential $|\chi_b|$ increases with increasing ion temperature, and that this effect is more pronounced in the intermediate and high pressure regimes ($L/\lambda_i > 1$). Similar results were obtained by Sternovsky and Robertson (see Ref. 6, Figs. 2 and 3).

VI. ANALYSIS OF THE PLASMA POTENTIAL EQUATION

The normalized plasma potential is given by the solution of Eq. (8) with a reference potential at the origin of coordinates $\chi(0) = 0$. This solution can be written in the form

$$\chi = \ln(h) + (1+\tau)\delta \cdot s_b \int_0^{s/s_b} u d(s/s_b) + (m_e/M)(1+\tau)u^2/2. \tag{10}$$

The third term in the right hand side of Eq. (10) is clearly negligible. The integral $I_u(s/s_b) \equiv \int_0^{s/s_b} u d(s/s_b)$ represents

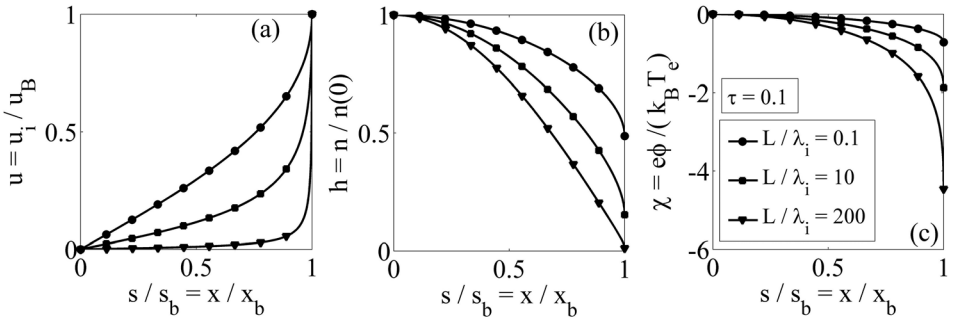

FIG. 2. Distribution of normalized (a) ion fluid velocity u, (b) plasma density h, and (c) plasma potential χ for different values of L/λ_i (planar case).

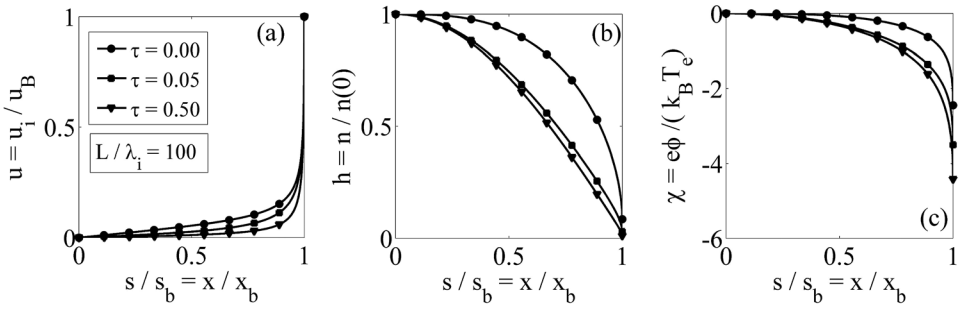

FIG. 3. Distribution of normalized (a) ion fluid velocity u, (b) plasma density h, and (c) plasma potential χ for different ratios $\tau = T_i/T_e$ (planar case).

the area under the graph of u vs. s/s_b, and one can see in Fig. 2(a) that $0 < I_u < 0.5$, and $I_u \to 0$ in the large pressure regime ($L/\lambda_i \gg 1$). In addition, one can see in Fig. 4(a) that $0 < s_b < 2$, and $s_b \to 0$ for $L/\lambda_i \gg 1$. Finally, as was discussed in Sec. III, one always has $\delta \ll c$, and according to Fig. 1, $c < 1$ in the low pressure regime and can reach large values (of the order of 10^6) in the high pressure regime. Therefore, $\delta \ll 1$ at low pressures and can reach large values ($\ll 10^6$) in the intermediate and high pressure regimes. Thus, it follows that the product of the three factors $\delta \cdot s_b \cdot I_u$ is negligible in both, the low and high pressure regimes, and can be slightly significant only in some range of intermediate pressures in which δ could be relatively large and the product $s_b \cdot I_u$ is not too small. Therefore, neglecting the second and third terms in the right hand side of Eq. (10), i.e., assuming Boltzmann distribution $h = e^{\chi}$, for the plasma electrons can be considered as a good approximation.

VII. COMPARISON WITH THE VARIABLE MOBILITY MODEL

In the case of parallel plates, one has $\beta = 0$, and Eqs. (6) and (7) can be combined to obtain

$$\frac{1}{h}\frac{dh}{du} = -\frac{2u + cu\sqrt{\theta + u^2}}{1 + u^2 + cu^2\sqrt{\theta + u^2}}. \tag{11}$$

The solution of Eq. (11) with initial condition $h(0) = 1$ can be written in the form

$$h(u) = \frac{\exp[-f(u)]}{[1 + u^2 + cu^2\sqrt{\theta + u^2}]^{\alpha}}. \tag{12}$$

In Eq. (12), the parameter $\alpha > 0$ is a constant to be determined later. By substituting Eq. (12) in Eq. (11), one obtains

$$f(u) = \int_0^u \frac{[2(1-\alpha) + [(1-2\alpha)\theta c + (1-3\alpha)cu^2](\theta + u^2)^{-1/2}]}{1 + u^2 + cu^2\sqrt{\theta + u^2}} u du. \tag{13}$$

The parameter α can be selected in such a way that $f(u) > 0$ for all possible values of the parameters $c = \pi u_B/(2\lambda_i \nu_{iz})$ and $\theta = 2T_i/(T_e + T_i)$, and one sees in Eq. (13) that this is achieved when $0 < \alpha \le 1/3$. The selection of $\alpha = 1/3$ leads to

$$f(u) = \frac{1}{3}\int_0^u \frac{4u + \theta cu(\theta + u^2)^{-1/2}}{1 + u^2 + cu^2\sqrt{\theta + u^2}} du. \tag{14}$$

The plasma density at the plasma sheath boundary $h_b \equiv h(1)$ is, therefore, given by

$$h_b = e^{-f(1)}[2 + c\sqrt{\theta + 1}]^{-1/3}. \tag{15}$$

In Fig. 6, the dependence of the factor $e^{-f(1)}$ on the pressure regimes and on the ion temperature is shown.

The variable mobility model[5] in which cold ions is assumed ($T_i = 0 \Rightarrow \theta = 0$) and the ion inertia is neglected leads to

$$h_b = [1 + c]^{-1/3}. \tag{16}$$

Because $0 < e^{-f(1)} < 1$ according to Fig. 6, one obtains that at the plasma-sheath boundary, the plasma density given by

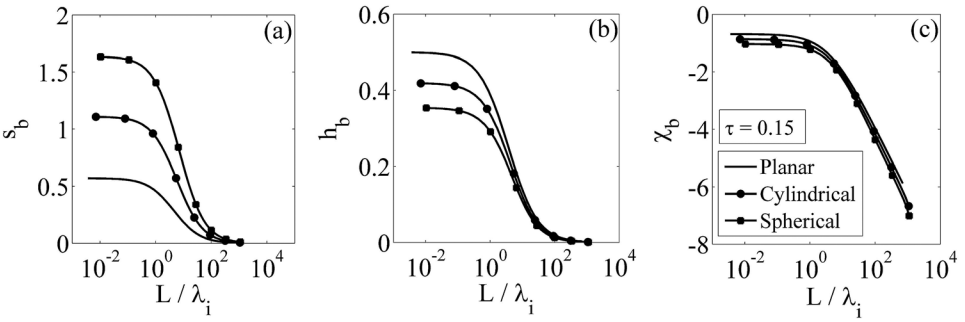

FIG. 4. Comparison of the dependence of the normalized (a) Plasma-sheath boundary location s_b, (b) plasma density h_b, and (c) plasma potential χ_b on L/λ_i for the planar, cylindrical, and spherical geometries.

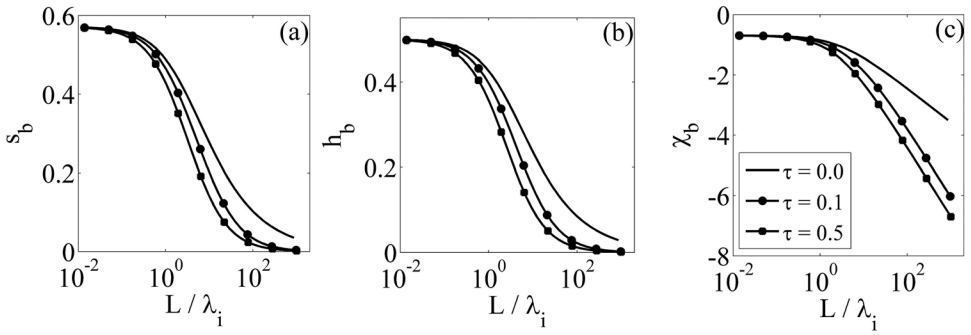

FIG. 5. Comparison of the dependence of the normalized (a) Plasma-sheath boundary location s_b, (b) plasma density h_b, and (c) plasma potential χ_b on L/λ_i for different values of the ratio $\tau = T_i/T_e$ (planar geometry).

Eq. (15) is lower than that predicted by the variable mobility model that is given by Eq. (16). Thus, one concludes that the combined effect of nonzero ion temperature and ion inertia causes a decrease in the plasma density at the plasma sheath boundary. In addition, one sees in Fig. 6 that at intermediate and high pressures ($L/\lambda_i > 1$), the assumption $T_i = 0$ is not justified even for $\tau < 0.1$.

VIII. COMPARISON WITH THE CURRELI AND CHEN'S MODEL

Curreli and Chen's recent model[2] considers plasma immersed in an external magnetic field and confined by a cylinder having a length much larger than its radius; the plasma parameters depend on the radius. This model takes into account several physical effects, including local ionization, short circuit effect, neutral depletion, and radio frequency heating. In the present paper, we consider a simpler model of the plasma without a magnetic field and with radial variation only in the plasma density, potential, and ion drift velocity, while the plasma electron temperature and neutral gas density are assumed to be constant values. The present model is focused on three main issues: (a) the appropriate limits of ion dynamics at low pressure ($R/\lambda_i < 1$) where $\nu_{in} \propto u_i$, and high pressure ($R/\lambda_i > 1$) where $\nu_{in} \propto \sqrt{k_B T_i/M}$ are expected; (b) the influence of nonzero ion temperature on the distribution of the plasma parameters; and (c) the unified treatment of the plasma planar, cylindrical, and spherical geometries. The results of the present model will be compared only with the results reported in the

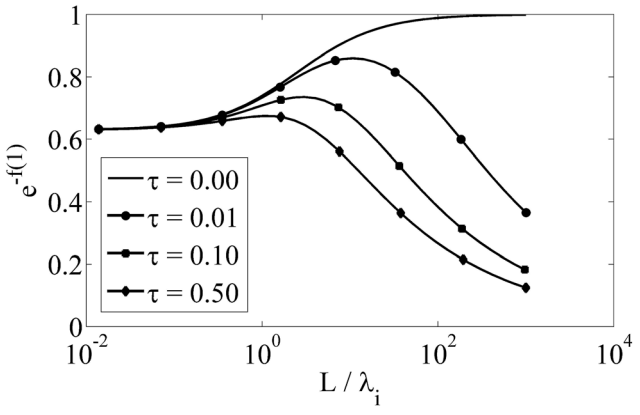

FIG. 6. Exponential factor at different values of L/λ_i for different ratios $\tau = T_i/T_e$.

preliminary sections of Ref. 2, where the simpler case we are considering was addressed (Ref. 2, Secs. II–IV and VI).

The differential equation [Ref. 2, Eq. (20)] for the radial ion drift velocity is

$$\frac{du}{ds} = \frac{1}{1-u^2}\left[1 + ku^2 - \frac{u}{s}\right];\ k = 1 + \frac{\nu_{in}}{\nu_{iz}}. \tag{17}$$

This equation differs from Eq. (6) in the expression for the ion-neutral collision frequency ν_{in}. Let us note that if one considers $k = \text{Const}$, then k^{-1} will be equivalent to the parameter A used by Self and Ewald in Ref. 3. In this particular case, Eqs. (20) and (25) described in [Ref. 2, Secs. IV and VI] coincide with Self and Ewald's model. However, it has to be remembered that, in Ref. 2, the parameter k is in general a function of the radial coordinate and not a constant, as Self and Ewald considered.

In the present paper, the parameter k depends implicitly on the radius through the dependence of the ion-neutral collision frequency ν_{in} on the ion drift velocity, while in Ref. 2, the dependence of k on the radius is stronger, because the ionization frequency ν_{iz} is calculated using local conditions. In Ref. 2, the ion-neutral collision frequency is given by $\nu_{in}(r) = n_n \sigma_{cex}(E_i) u_i(r)$, where the ion energy is $E_i = 0.5 M u_i^2(r)$ (plus a contribution of the ion thermal energy near the axis), and the charge exchange cross section dependence on ion energy is given by a fitting of experimental data (for Ar gas). In the present work, Wannier's expression is used to calculate the ion-neutral collision frequency. In this expression, the ion thermal energy is taken into account not in the charge-exchange cross section but in the ion velocity [see Eq. (4)]. Let us note that, in the case of cylindrical geometry, near the axis one expects $\nu_{in} \propto T_i^{1/2}$, while near the plasma boundary one expects $\nu_{in} \propto u_i$. By using Wannier's expression [Eq. (4)] for ion-neutral collisions, the broad range of pressure, i.e., low−intermediate−high pressure regimes, as well as the change in ion-neutral collisionality experienced by the ions while traveling toward the wall, are matched in an explicit and consistent manner. Applying Eq. (4), it is found that the normalized ion velocity $u = u_i/u_B$, plasma density $h = n(r)/n(0)$, and plasma potential $\chi = e\varphi/(k_B T_e)$, have an "universal behavior" similar to those obtained in Ref. 2. Namely, the distributions of these plasma parameters (with respect to the normalized coordinate $s/s_b = r/R$) are independent of the radius$R$ of the cylinder, the plasma density at the axis $n(r = 0) = n(0)$, and the neutral density n_0. In addition to the model,[2] the results of

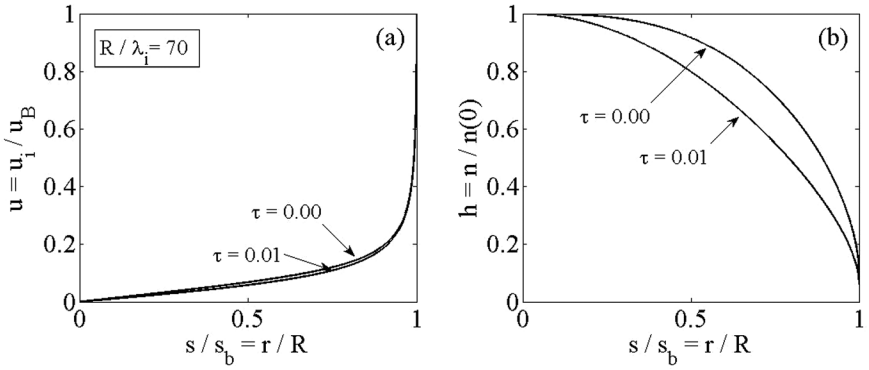

FIG. 7. Influence of ion temperature in the radial distribution of normalized (a) ion velocity and (b) plasma density.

the present model showed that this "universal behavior" of the plasma parameters does depend on the parameter $R/\lambda_i \equiv Rn_0\sigma_{cex}$ (see Figs. 4(a), 2(a), and 2(c)) and on the ratio $\tau = T_i/T_e$ (see Figs. 3(a)–7). Also, a unified treatment of parallel plates, cylindrical, and spherical geometry are given in the present model, while in Ref. 2, only the cylindrical case was considered.

In the model,[2] the diffusion term $k_B T_i \nabla n$ was neglected assuming that, in almost all of the applications, one finds that $T_i/T_e \equiv \tau \ll 1$. However, the results of the present model [see Fig. (7)] showed the different distributions of the plasma density obtained either by assuming $T_i = 0$ $(\tau = 0)$, or by assuming $T_i \neq 0$ with $T_i \ll T_e$ $(\tau = 0.01)$.

Thus, considering $T_i > 0$ produces a non-negligible effect on the plasma density distribution, even for $T_i \ll T_e$. In addition, the plasma within Orificed Hollow Cathodes used in ion thrusters (see Sec. XI) is characterized by significant temperature of ions and neutrals, which can be of the order of several thousand Kelvin degrees [Ref. 16, p. 258, 466] leading to $T_i/T_e \equiv \tau \geq 0.1$. One also can see in Fig. 11 in Sec. XI that the electron temperature is sensitive to $T_i \neq 0$, especially at low pressures.

IX. COMPARISON WITH EARLIER MODELS

Several models were based on the same set of differential equations; they differ in the assumptions regarding plasma collisionality, ion temperature, and the additional considerations made in order to simplify the equations. In Table I, the plasma density distribution predicted by several models are compared.

Here, the coefficient $D_a \approx k_B(T_i + T_e)/(M\nu_{in})$ is the ambipolar diffusion coefficient. The variable mobility model was analyzed in Sec. VII and the Curreli and Chen model[2] was briefly described in Sec. VIII. The "cold ion" model described in Ref. 14 is a collisionless ("free fall") model and is valid in the low pressure regimes $(L/\lambda_i \ll 1)$. This can be obtained from the solution given in the last line in Table I, because at low pressures $c \to 0$ (see Fig. 1) and the exponential factor $e^{-f(u)}$ becomes the factor $[1+u^2]^{-2/3}$, as can be verified by integrating Eq. (14). The Self and Ewald model[3] assumes that the ion-neutral collision frequency does not depend on the ion fluid velocity in all of the pressure range; the coefficients β_1, β_2 in this model can be found in Ref. 3, Eq. (18).

TABLE I. Comparison of the plasma density distribution predicted by several models (planar geometry).

Model's name	Plasma density distribution
Variable mobility (Ref. 4)	$n(u) = n(0)[1+cu^3]^{1/3}$
Ambipolar diffusion (Ref. 6)	$n(x) = n(0)\cos[(\nu_{iz}/D_a)^{1/2}x]$
Cold ions (Ref. 13)	$n(u) = n(0)[1+u^2]^{-1}$
Self and Ewald (Ref. 2)	$n(u) = n(0)[1+\beta_1 u^2]^{-\beta_2}$
New model	$n(u) = n(0)e^{-f(u)}[1+u^2+cu^2\sqrt{\theta+u^2}]^{-1/3}$

Sternovsky and Robertson's model[6] has no analytical solution for plasma density distribution and it was not included in Table I, but the results of their model are similar to those found in Sec. V in the present paper. The ambipolar diffusion model,[7] which is valid in the large pressure regime $(L/\lambda_i \gg 1)$, is the only model that gives an explicit dependence of the plasma density on the spatial coordinate, while all the other models depend on the ion fluid velocity, which in turn is related to the spatial coordinate in a nonlinear implicit manner.

One can also compare the values of h_b given by Eq. (15) with those given by the following heuristic expression for the plasma density in the planar case:[8]

$$h_b \approx 0.86\left[3 + \frac{L}{\lambda_i} + \frac{4}{5}\tau\left(\frac{L}{\lambda_i}\right)^2\right]^{-1/2}. \quad (18)$$

The results are compared in Fig. 8. One can see that there is relatively good agreement between the two models.

The case of cylindrical geometry was shown in Fig. 4(a) and can be compared with the solution shown in Fig. 3 in Ref. 3. It has to be noted that the parameters c and s_b in the present study correspond, respectively, to the parameters A and $A \cdot s_b$ in Ref. 3, but $c \gg 1$ is equivalent to $A \to 0$, while $c \to 0$ is equivalent to $A \to 1$. These differences appear because of the assumed constant ion-neutral collision frequency considered in Ref. 3, which results in different normalizations for the plasma sheath boundary location s_b. This comparison showed that the qualitative behavior of s_b at low pressure is different, i.e., tending to be constant, in the present model, whereas in Ref. 3, the normalized sheath boundary position always increases with decreasing gas pressure. This observation, along with the expression for s_b given in Eq. (9) in the present paper, implies that, at low pressures, the electron temperature in the present model is more sensitive to changes in the gas pressure than as presented in Ref. 3.

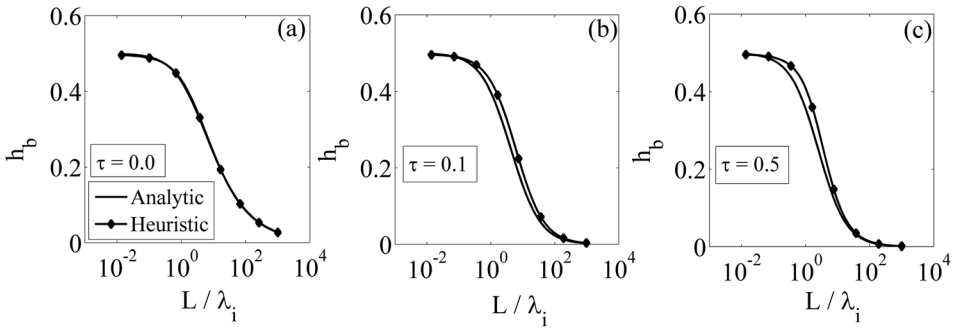

FIG. 8. Comparison of the plasma density distribution predicted by the heuristic expression given in Eq. (17) with the analytical solution Eq. (15) at different values of the ratio $\tau = T_i/T_e$ (planar geometry).

X. ANALYTICAL SOLUTION IN PLANAR GEOMETRY

There are no analytical solutions for Eqs. (6) and (11) because of the square root terms. However, an approximated analytical solution can be found if the square root terms are temporarily substituted by an appropriate polynomial expression. It was found that this solution includes the polynomial expression, thus allowing substitution back to the original square root. It can be seen that the ion-neutral collision frequency Eq. (5) always appears in Eqs. (6) and (11) multiplied by either u or u^2, giving rise to functions of the form $g_N(u,\theta) = u^N\sqrt{\theta+u^2}$ for $N = 1, 2$; these functions can be approximated by the polynomial functions $\tilde{g}_N(u,\theta) = u^N[A_N(\theta) + B_N(\theta)u]$, where $A_N(\theta), B_N(\theta)$ are fitting coefficients. The functions satisfy $g_N(0,\theta) = \tilde{g}_N(0,\theta) = 0$. In order to find $A_N(\theta)$ and $B_N(\theta)$, the following boundary condition is used:

$$\tilde{g}_N(1,\theta) = g_N(1,\theta) \iff A_N(\theta) + B_N(\theta) = \sqrt{\theta+1}. \quad (19)$$

The function $g_N(u,\theta)$ is related to the energy losses of the ion flow. Thus, the integral of the function $\tilde{g}_N(u,\theta)$ within the interval $0 \le u \le 1$ should give the same result as the integral of the function $g_N(u,\theta)$ in the same interval

$$\int_0^1 u^N[A_N(\theta) + B_N(\theta)u]du = \int_0^1 u^N\sqrt{\theta+u^2}du \equiv I_N(\theta). \quad (20)$$

Equations (19) and (20) are sufficient to determine the fitting coefficients, the result of which is

$$A_1(\theta) = 6I_1(\theta) - 2\sqrt{\theta+1}, \quad B_1(\theta) = 3\sqrt{\theta+1} - 6I_1(\theta), \quad (21)$$

$$I_1(\theta) = (1/3)[(\theta+1)^{3/2} - \theta^{3/2}], \quad (22)$$

$$A_2(\theta) = 12I_2(\theta) - 3\sqrt{\theta+1}, \quad B_2(\theta) = 4\sqrt{\theta+1} - 12I_2(\theta), \quad (23)$$

$$I_2(\theta) = (1/4)(\theta+1)^{3/2} - (1/8)\theta(\theta+1)^{1/2} - (1/8)\theta^2\ln[\theta^{-1/2} + \theta^{-1/2}(\theta+1)^{1/2}]. \quad (24)$$

The analytical solution of Eqs. (6) and (11), found with help of the fitting polynomials, is given by

$$s \approx -\frac{1}{cB_2}\left\{\left(\frac{1+A_s}{2}\right)\Omega_1(u) - \left(\frac{1+3A_s}{2}\right)\Omega_2(u) - \frac{(4w_2 - 3z_1 - 9z_1A_s)}{3\sqrt{3z_1^2 - 4w_2^2/3}}[\Omega_3(u) - \Omega_3(0)]\right\}, \quad (25)$$

$$\ln(h) \approx -\frac{B_1}{B_2}\left\{\left(\frac{1-A_h}{2}\right)\Omega_1(u) + \left(\frac{3A_h-1}{2}\right)\Omega_2(u) + \frac{3z_1 - 4w_2 + 6w_1 - 9z_1A_h}{3\sqrt{3z_1^2 - 4w_2^2/3}}[\Omega_3(u) - \Omega_3(0)]\right\}, \quad (26)$$

$$\chi \approx \ln(h). \quad (27)$$

The functions Ω are

$$\Omega_1(u) = \ln\left[1 + u^2 + cu^2\sqrt{\theta+u^2}\right], \quad (28)$$

$$\Omega_2(u) = \ln|(3u + w_2 - 3z_1)/(w_2 - 3z_1)|, \quad (29)$$

$$\Omega_3(u) = \tan^{-1}\left[\frac{2u + z_1 + 2w_2/3}{\sqrt{3z_1^2 - 4w_2^2/3}}\right]. \quad (30)$$

The coefficients are

$$A_s = [1 - (z_1 - w_2/3)^2]/(3z_1^2 - w_2^2/3), \quad (31)$$

$$A_h = (z_1 - w_2/3)(z_1 - w_2/3 + w_1)/(3z_1^2 - w_2^2/3), \quad (32)$$

$$z_1 = \left[-(q/2) + \sqrt{(q^2/4) - (w_2^6/27^2)}\right]^{1/3} + \left[-(q/2) - \sqrt{(q^2/4) - (w_2^6/27^2)}\right]^{1/3}, \quad (33)$$

$$w_1 = \frac{2 + cA_1}{cB_1}; \quad w_2 = \frac{1 + cA_2}{cB_2}; \quad q = 1/(cB_2) + 2w_2^3/27. \quad (34)$$

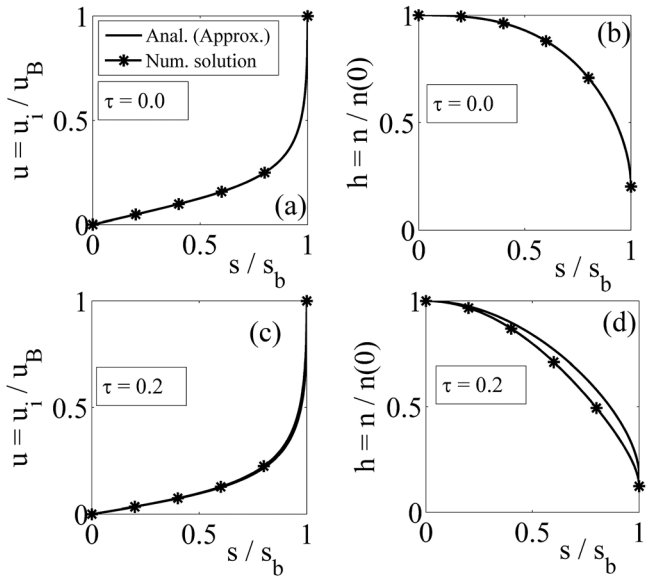

FIG. 9. Comparison of the analytical and numerical solutions of Eqs. (6) and (11) for normalized (a) ion fluid velocity u at $\tau = 0$, (b) plasma density h at $\tau = 0$, (c) ion fluid velocity u at $\tau = 0.2$, and (d) plasma density h at $\tau = 0.2$.

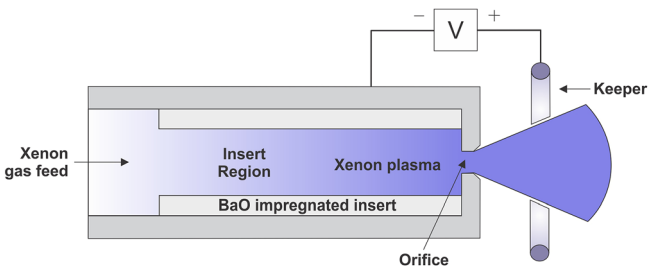

FIG. 10. Schematic of a Hollow cathode.

In Fig. 9, the normalized ion fluid velocity and plasma density obtained from Eqs. (25) and (26) are compared with the numerical solution of Eqs. (6) and (11), respectively. For $\tau = 0$ ($T_i = 0$), both solutions coincide (see Figs. 9(a) and 9(b)) because in that case exact analytic solution of Eqs. (6) and (11) exist. For $\tau \neq 0$, the analytical solution for $s(u)$, Eq. (25), is a good approximation (see Fig. 9(c)), while the analytical solution for h, Eq. (26), exhibits slightly larger values than the numerical solution (see Fig. 8(d)).

XI. APPLICATIONS TO HOLLOW CATHODES

Hollow cathodes are known to be one of the best high current plasma sources and are one of the critical components of most electrostatic and Hall ion thrusters used in space applications where these cathodes provide electrons to neutralize the ion beam and/or to ionize the propellant. Hollow cathodes for space applications usually consist of a metal tube impregnated in its interior with a low work function material (thermo-emitter) and capped at one side by a plate with a small orifice, as shown in Fig. 10. The propellant (usually xenon gas) fed to the cathode is ionized in the so-called insert region by electrons emitted by the thermo-emitter. These electrons gain the necessary energy from the potential drop sustained between the anode (in this case, the anode is a keeper biased positively with respect to the insert) and the thermo-emitter. The plasma generated by the ionization of the neutral gas expands from the insert region through a small orifice designed to prevent the thermo-emitter from severe ion bombardment back streaming from the outer plasma. The inner diameter of the insert region is commonly small (several millimeters), and the gas flows so slowly that the ion dynamics is mainly in the radial direction.

The present model will be applied to the NEXIS Hollow Cathode[16] used in space applications, which has inner radius $R = 0.635\,\text{cm}$ and operates with xenon gas. The mass of the Xe atom is $M = 2.18 \times 10^{-25}\,\text{kg}$, and it has ionization energy $U_{iz} = 13.1\,\text{eV}$. According to Goebel and Katz,[16] the following approximation for the ionization frequency is valid for $T_e \leq 5\,\text{eV}$:

$$\nu_{iz} \approx n_0 \langle \sigma_{iz} \rangle \sqrt{8eT_e/(\pi m_e)}, \tag{35}$$

$$\langle \sigma_{iz} \rangle \approx 10^{-20}[3.97 + 0.643T_e - 0.0368T_e^2]e^{-U_{iz}/T_e}. \tag{36}$$

Here, the units of T_e is electron volts, and that of σ_{iz} is square meters. The ion-neutral collisions are dominated by charge exchange processes, and therefore the cross section is $\sigma_{in} \approx \sigma_{cex} \approx 10^{-18}\,\text{m}^2$ (Refs. 16 and 17) and the ion mean free path is $\lambda_i = (n_0\sigma_{cex})^{-1}$. One can thus write

$$c \approx 2 \times 10^{-3}(1+\tau)^{1/2}\sigma_{cex}/\langle \sigma_{iz} \rangle. \tag{37}$$

Equations (35)–(37) are used along with Eqs. (6), (7), and (9) to obtain the dependence of the electron temperature on the gas pressure, as shown in Fig. 11.

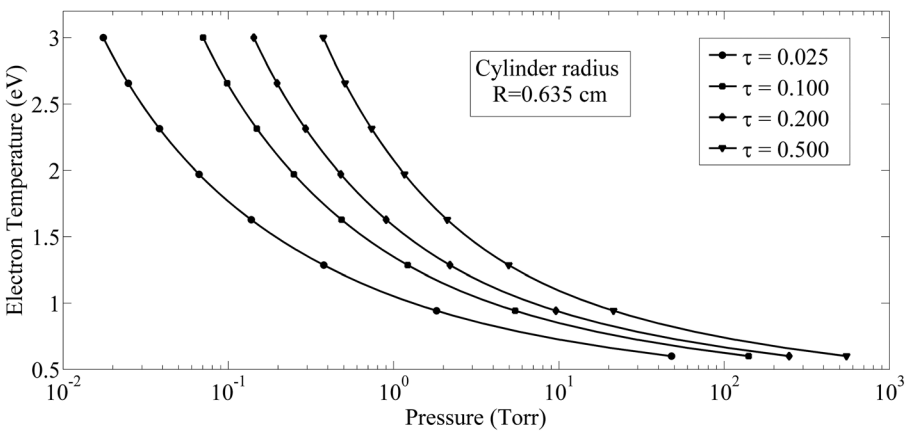

FIG. 11. Electron temperature vs. pressure for different values of the ratio $\tau = T_i/T_e$.

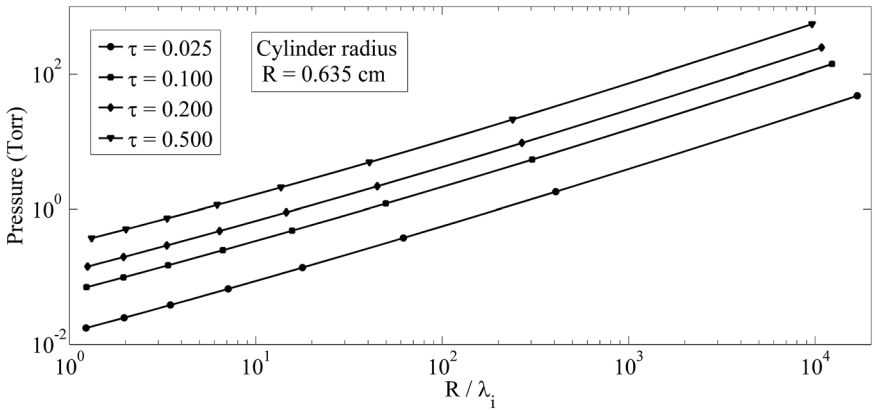

FIG. 12. Dependence of the neutral gas pressure on R/λ_i for different values of $\tau = T_i/T_e$.

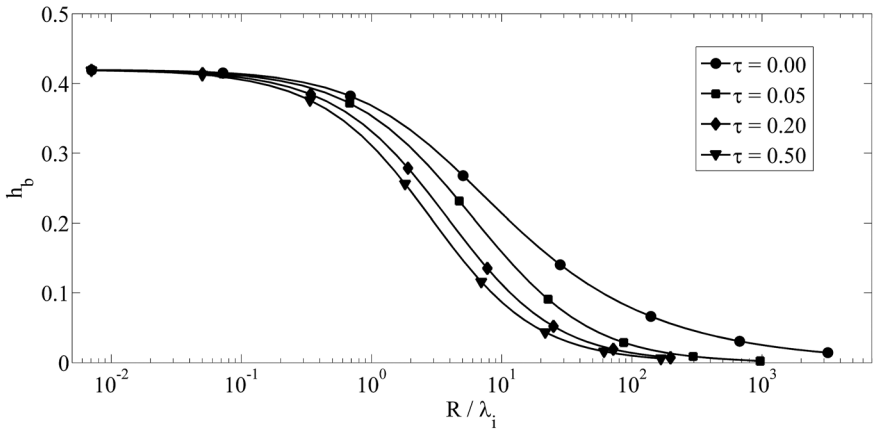

FIG. 13. Dependence of the normalized plasma density at the plasma-sheath boundary on the pressure regime for different values of $\tau = T_i/T_e$.

The ratio R/λ_i, which determines the pressure regime, is related to the neutral pressure as shown in Fig. 12. Because of the log-log scale, one can infer that there is a relation of the form $P_0 \approx a(R/\lambda_i)^b$, where a is dependent on τ, and b is a positive constant.

As discussed in Sec. V, the value of $h_b = J_{i,b}/(en(0)u_B)$ represents the normalized ion current density flowing out of the plasma toward the inner wall of the insert. Fig. 13 shows that in the range $1 < R/\lambda_i < 100$, the ion current density toward the wall strongly depends on the ion temperature, while for $R/\lambda_i < 0.2$, it is approximately independent of it. In addition, one sees in Fig. (13) that the ion current density toward the wall is strongly reduced with increasing plasma collisionality.

XII. CONCLUSIONS

The proposed plasma model describes in a unified manner the behavior of plasma's parameters in the low, intermediate, and high pressure regimes. It was found that the electron inertia has no appreciable effect on the dynamics of the plasma particles, while the combined effect of ion inertia and nonzero ion temperature results in reducing the plasma density, increasing the plasma potential, and reducing the ion current density entering the sheath region. It was also found that the ion temperature cannot be neglected even when $\tau \equiv T_i/T_e < 0.1$.

ACKNOWLEDGMENTS

We would like to thank Valery Godyak, Yury Bliokh, and Tal Queller for useful discussions.

[1]F. F. Chen, *Introduction to Plasma physics and Controlled fusion* (Springer, New York, 2006), Vol.1, p. 77.
[2]D. Curreli and F. F. Chen, Phys. Plasmas **18**, 113501 (2011).
[3]S. A. Self and H. N. Ewald, Phys. Fluids **9**, 2486 (1966).
[4]L. Tonks and I. Langmuir, Phys. Rev. **34**, 876 (1929).
[5]V. A. Godyak, *Soviet Radio Frequency Discharge Research* (Delphic Associates, 1986), p. 79.
[6]Z. Sternovsky and S. Robertson, IEEE Trans. Plasma Sci. **34**(3), 850 (2006).
[7]W. Schottky, Phys. Z **25**, 635 (1924).
[8]P. Chabert and N. Braithwaite, *Physics of Radio-Frequency Plasmas* (Cambridge University Press, N.Y., 2011), p. 59.
[9]M. A. Lieberman and A. J. Lichtemberg, *Principles of Plasma Discharges and Materials Processing* (John Wiley & Sons, Inc., N.J., 2005).
[10]C. Lee and M. A. Lieberman, J. Vac. Sci. Technol. A **13**, 368 (1995).
[11]P. Chabert, A. J. Lichtenberg, and M. A. Lieberman, Phys. Plasmas **14**, 093502 (2007).
[12]A. Fruchtman, in *Proceeding of the 33rd EPS Conference on Plasma Physics, Italy, 2006 ECA* (Rome, 2006), Vol. 30I, p. D-5.013.
[13]A. Fruchtman, IEEE Trans. Plasma Sci. **36**, 403 (2008).
[14]J. E. Allen, Plasma Sources Sci. Technol. **18**, 014004 (2009).
[15]G. H. Wannier, Bell Syst. Tech. J. **32**, 170 (1953).
[16]D. Goebel and I. Katz, *Fundamentals of Electric Propulsion* (John Wiley & Sons, N.J., 2008), p. 243.
[17]J. S. Miller, S. H. Pullins, D. J. Levandier, Y. Chiu, and R. A. Dressler, J. Appl. Phys. **91**, 984 (2002).